



# Characteristic, electrical and optical properties of potassium borate ( $\text{KB}_5\text{O}_8 \cdot 4\text{H}_2\text{O}$ ) hydrothermally synthesized from different boron sources

Fatma Tugce Senberber Dumanli<sup>1,2</sup> · Meral Yildirim Ozen<sup>1</sup> · Miguel Ortega Asensio<sup>3</sup> · Sureyya Aydin Yuksel<sup>4</sup> · Azmi Seyhun Kipcak<sup>1</sup> · Emek Moroydor Derun<sup>1</sup>

Received: 8 April 2021 / Accepted: 28 July 2021 / Published online: 11 August 2021  
© The Author(s), under exclusive licence to Springer Nature B.V. 2021

## Abstract

Potassium borate was hydrothermally synthesized from various boron minerals ( $\text{H}_3\text{BO}_3$ ,  $\text{B}_2\text{O}_3$ ,  $\text{Na}_2\text{B}_4\text{O}_7 \cdot 5\text{H}_2\text{O}$  and  $\text{Na}_2\text{B}_4\text{O}_7 \cdot 10\text{H}_2\text{O}$ ) at reaction conditions of 60–90 °C and 15–120 min. The synthesized potassium borate was identified as “santite ( $\text{KB}_5\text{O}_8 \cdot 4\text{H}_2\text{O}$ )” from the X-ray diffraction (XRD) analyses results. The specific band values between B and O atoms were characterized by Fourier transform infrared and Raman spectroscopies. Multiangular particles were generally observed in the range of 3.41  $\mu\text{m}$ –234.94 nm. The use of different boron sources affected the morphology. Higher reaction yields were determined in the use of boric acid ( $\text{H}_3\text{BO}_3$ ). Optical absorption of potassium borate minerals was approximately 340 nm. AC and DC electrical properties of materials were determined by using current–voltage and capacitance voltage characteristics. Electrical resistivity values of DC were found in the range of  $4.17 \times 10^8$ – $4.07 \times 10^{10}$   $\Omega$  cm, whereas dielectric constants of AC were between  $2 \times 10^5$  and  $2 \times 10^6$ .

**Keywords** Electrical properties · Optical properties · Potassium borates · Synthesis

✉ Emek Moroydor Derun  
moroydor@yildiz.edu.tr; moroydor@gmail.com

<sup>1</sup> Department of Chemical Engineering, Faculty of Chemical and Metallurgical Engineering, Yildiz Technical University, Davutpasa Campus, Davutpasa Street No.127, 34220 Esenler, Istanbul, Turkey

<sup>2</sup> Department of Civil Engineering, Nisantasi University, Istanbul, Turkey

<sup>3</sup> Department of Chemical Engineering, Universidad de Valladolid, Valladolid, Spain

<sup>4</sup> Department of Physics, Yildiz Technical University, Istanbul, Turkey

## Introduction

Metal borates are the complexes of the boron, hydrogen, oxygen and metal atoms. The common types of metal borates are found naturally on earth crust, while the specific types can be prepared in micro-/macro-scale. Those with water molecules locked inside their crystals are referred to as borate hydrates. As being additives, both hydrated and non-hydrated forms of metal borates are used in most of industrial applications such as glass, ceramics, nuclear, space-aviation, metallurgy, transportation, cosmetics and chemistry. Each kind of metal borate has notable features which make them preferable for different areas [1, 2].

As a sub-class of metal borates, the potassium borates are important among fields such as metal refining, welding, lubricating oil additives, cement, insulation, textiles, fibreglass and as a superior nonlinear optical material (NLO) against commonly used borate compounds. As a member of potassium borate family, potassium pentaborate ( $\text{KB}_5\text{O}_8 \cdot 4\text{H}_2\text{O}$ ) is also known as “santite” mineral. It has the orthorhombic lattice system, and its crystals are at the appearance of transparent and colourless aggregates. In the structure of  $\text{KB}_5\text{O}_8 \cdot 4\text{H}_2\text{O}$ , the large difference in the electronegativity values of B and O atoms is responsible for the high transmittance in the shorter wavelength region [3–7].

There are different types of prepared potassium borates in the system of  $\text{K}_2\text{O}-\text{B}_2\text{O}_3-\text{H}_2\text{O}$ . Zhang et al. obtained the  $\text{KB}_5\text{O}_7(\text{OH})_2\text{H}_2\text{O}$  by using the raw materials of potassium hydroxide (KOH), boric acid ( $\text{H}_3\text{BO}_3$ ) and pyridine at 170 °C for 7 days [8]. Salentine prepared the  $\text{KB}_3\text{O}_5 \cdot 3\text{H}_2\text{O}$  by the liquid state synthesis of  $\text{K}_2\text{B}_4\text{O}_7 \cdot 4\text{H}_2\text{O}$  and  $\text{KB}_5\text{O}_8 \cdot 4\text{H}_2\text{O}$  [9]. Wu synthesized the  $\text{K}[\text{B}_5\text{O}_7(\text{OH})_2]$  using the potassium nitrate ( $\text{KNO}_3$ ) and  $\text{H}_3\text{BO}_3$  at the reaction temperature 210 °C for 3 days [10]. Wang et al. produced the  $\text{KB}_3\text{O}_4(\text{OH})_2$  by the hydrothermal reaction of  $\text{K}_2\text{B}_4\text{O}_7 \cdot 4\text{H}_2\text{O}$ , DMF and  $\text{H}_2\text{O}$  at 165 °C for 10 days [11]. Liu et al. researched on the thermochemistry of the synthesized  $\text{K}_2\text{B}_5\text{O}_8(\text{OH})_2\text{H}_2\text{O}$  with using the raw materials of potassium carbonate ( $\text{K}_2\text{CO}_3$ ) and  $\text{H}_3\text{BO}_3$  in hydrothermal conditions at the reaction temperature 170 °C for 7 days [12]. Alicilar studied the flame retardation and smoke suppression efficiencies of potassium additives in styrene acrylic paints [13].

The determination of electrical and optical features of compound is essential for the nanophotonic devices, semiconductor materials, solar cells, laser and display applications [14–17]. In order to improve the usage of boron compounds and boron-doped materials in these industrial applications, determination of physical features of borates should be comprehensively detailed. Known with its good mechanical features, aluminium borate and lithium aluminium borate were characterized by Ike et al. [18, 19]. The research would like to contribute to the possible use of potassium borates in the use of electronic and optic applications. With this purpose, the synthesized potassium borates with different boron sources were chemically and physically characterized.

## Materials and methods

### Raw materials preparation and characterization

Potassium nitrate ( $\text{KNO}_3$ ), with the minimum purity of 99%, was purchased from Merck Chemicals (Merck KGaA, Darmstadt, Germany) and used without pre-treatment. Boric acid ( $\text{H}_3\text{BO}_3$ ), boron oxide ( $\text{B}_2\text{O}_3$ ), tincalconite ( $\text{Na}_2\text{B}_4\text{O}_7 \cdot 5\text{H}_2\text{O}$ ) and borax ( $\text{Na}_2\text{B}_4\text{O}_7 \cdot 10\text{H}_2\text{O}$ ) were retrieved from Bandırma Boron Works (Eti Maden, Balıkesir, Turkey) at a particle size of 2 mm with the minimum purities of 98%. In order to maintain a particle sized below 75  $\mu\text{m}$ , boron sources were ground with Retsch RM 100 (Retsch GmbH & Co KG, Haan, Germany) agate mortar and sieved through Fritsch analysette 3 Spartan pulverisette 0 vibratory sieve-shaker (Fritsch, Idar-Oberstein, Germany).

Characterization of the raw materials was conducted by PANalytical X'pert Pro (PANalytical B.V., Almelo, The Netherlands) XRD with the generator settings of 45 kV and 40 mA. In the XRD analysis, Cu-K $\alpha$  ( $\lambda = 1.53 \text{ cm}^{-1}$ ) radiation is used and the  $2\theta$  range is selected from 10 to 90°.

### Synthesis procedure

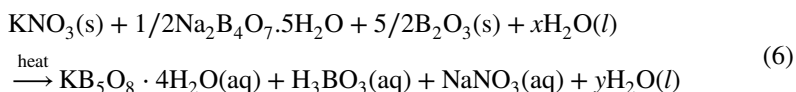
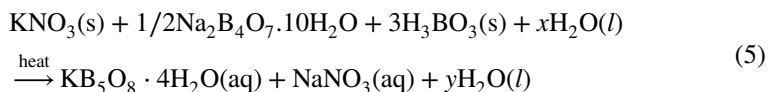
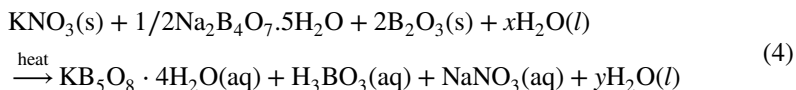
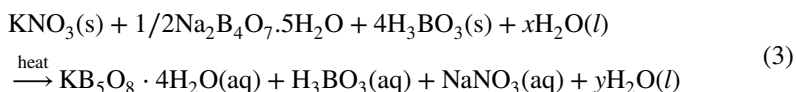
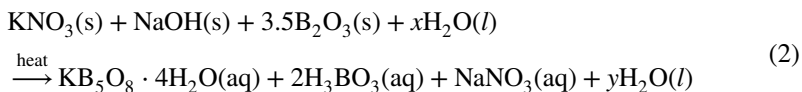
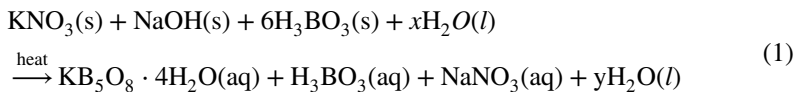
In the production of potassium borates, six different raw materials were reacted at different molar ratios, which were determined from pre-experiments given in Table 1. For all of the sets, the potassium source was used as KN ( $\text{KNO}_3$ ). Sodium source was used as Na (NaOH) in Set 1 and Set 2. The boron sources were used as H ( $\text{H}_3\text{BO}_3$ ) in Set 1, Set 3 and Set 5 and B ( $\text{B}_2\text{O}_3$ ) in Set 2, Set 4 and Set 6. T ( $\text{Na}_2\text{B}_4\text{O}_7 \cdot 5\text{H}_2\text{O}$ ) and Bx ( $\text{Na}_2\text{B}_4\text{O}_7 \cdot 10\text{H}_2\text{O}$ ) were used as both sodium and boron sources in Set 3, Set 4 and Set

**Table 1** Amount of raw materials that were used in the synthesis of potassium borates

Raw material*	Mole					
	Set 1	Set 2	Set 3	Set 4	Set 5	Set 6
KN	0.0216	0.0185	0.0210	0.0210	0.0210	0.0210
N	0.0216	0.0185	–	–	–	–
H	0.1294	–	0.0842	–	0.0630	–
B	–	0.0646	–	0.0420	–	0.0525
T	–	–	0.0105	0.0105	–	–
Bx	–	–	–	–	0.0105	0.0105
K:B ratio (mole/mole)	6	7	6	6	5	7

KN:  $\text{KNO}_3$ , N: NaOH, H:  $\text{H}_3\text{BO}_3$ , B:  $\text{B}_2\text{O}_3$ , T:  $\text{Na}_2\text{B}_4\text{O}_7 \cdot 5\text{H}_2\text{O}$ , Bx:  $\text{Na}_2\text{B}_4\text{O}_7 \cdot 10\text{H}_2\text{O}$

5, Set 6, respectively. The reaction temperatures and times were determined between 90 and 60 °C and 120–15 min, respectively. Expected reactions are given in (1) to (6):



During the synthesis, 100-mL batch-type temperature-controlled glass reactor was used. Distilled water obtained from GFL 2004 (Gesellschaft für Labortechnik, Burgwedel, Germany) water purification system was used for the reaction medium. In the experiments, the boron sources were added to reactor and after the determined temperature is reached, the potassium and sodium sources were added to medium. After the determined reaction time was reached, reactor contents were placed in a glass crystallizer at 40 °C in an oven (Ecocell LSIS-B2V/EC55; MMM Medcenter Einrichtungen, Planegg, Germany) in order to evaporate the excess water and for crystallization to occur. After the crystals were formed, the sample was washed with pure ethanol to remove the unreacted raw materials formed by NaNO<sub>3</sub>. Then, excess ethanol was removed by putting the washed sample in an oven which was heated to 40 °C.

### Characterization of the synthesized products

After the liquid state synthesis of potassium borates, the samples were characterized by XRD, FT-IR and Raman spectroscopy techniques. The XRD parameters used in Sect. 2.1 for the raw material preparation and characterization were the same,

including the  $2\theta$  range, where the characteristic peaks of potassium borates were observed.

The FT-IR analyses was done by PerkinElmer, MA, USA, with a universal attenuation total reflectance (ATR) sampling accessory coupled to a diamond/ZnSe crystal. The Raman analysis was done by using Raman spectrometer of model PerkinElmer Raman Station 400F (PerkinElmer, CT, USA). The characteristic vibrations of both FT-IR and Raman spectra analyses were at the range of  $1800\text{--}650\text{ cm}^{-1}$  and  $1600\text{--}250\text{ cm}^{-1}$ , respectively.

The surface morphologies and particle sizes of the samples were investigated by using CamScan brand Apollo 300 field-emission SEM (CamScan, Oxford, UK) at 15 kV. The detector used was backscattering electron (BEI), and the magnification was set to 5,000.

Three parallel experiments for each formation were conducted for the santite yield calculations.  $\text{KNO}_3$  was selected as the key component (limiting reactant), and the equation used in the calculation is given below:

$$Y_{\text{Santite}} = \frac{N_{\text{Santite}}}{\left(N_{\text{KNO}_3}\right)_i - \left(N_{\text{KNO}_3}\right)_f} \quad (7)$$

where  $Y_{\text{Santite}}$  is the yield of santite,  $N_{\text{Santite}}$  is the final formation mole of santite, and  $(N_{\text{KNO}_3})_i$  and  $(N_{\text{KNO}_3})_f$  are the moles of  $\text{KNO}_3$  initial and final, respectively.

## Electrical and optical properties

The potassium borates powder which have the highest XRD scores were pressed under pressure of 30 MPa into pellets to 13 mm diameters. Electrical resistivity of the samples was measured with current–voltage technique at room temperature

**Table 2** XRD results and crystallographic data of the raw materials used and produced potassium borate

Compound	Pdf code	Mineral name	Mineral formula	Crystal system [Space Gr./No.]	a (Å), b (Å), c (Å) [ $\alpha$ (°), $\beta$ (°), $\gamma$ (°)]
KN	00-005-0377	Nitre	$\text{KNO}_3$	Orthorhombic [Pmcn/62]	5.41, 9.16, 6.43 [90.0, 90.0, 90.0]
H	01-073-2158	Sassolite	$\text{H}_3\text{BO}_3$	Anorthic [P-1/2]	7.04, 7.05, 6.58 [92.6, 101.2, 119.8]
B	00-006-0297	Boron oxide	$\text{B}_2\text{O}_3$	Cubic [P E/n.a.*]	10.06, 10.06, 10.06 [90.0, 90.0, 90.0]
T	00-007-0277	Tinalconite	$\text{Na}_2\text{B}_4\text{O}_7 \cdot 5\text{H}_2\text{O}$	Rhombohedral [R-3/148]	11.12, 11.12, 21.20 [90.0, 90.0, 120.0]
Bx	01-075-1078	Borax	$\text{Na}_2\text{B}_4\text{O}_7 \cdot 10\text{H}_2\text{O}$	Monoclinic [C2/c]	11.89, 10.65, 12.21 [90.0, 106.6, 90.0]
KB	01-072-1688	Santite	$\text{KB}_3\text{O}_8 \cdot 4\text{H}_2\text{O}$	Orthorhombic [Aba2/41]	11.06, 11.18, 9.04 [90.0, 90.0, 90.0]

\* n.a.: not available in the pdf card

**Table 3** XRD scores of the potassium borates synthesized from different raw materials

Reaction Temperature (°C)	Reaction Time (min)	Set 1 (KN-N-H)	Set 2 (KN-N-B)	Set 3 (KN-T-H)	Set 4 (KN-T-B)	Set 5 (KN-Bx-H)	Set 6 (KN-Bx-B)
60	15	42	53	64	63	64	63
60	30	60	60	69	53	69	47
60	60	<b>75</b>	<b>72</b>	<b>77</b>	56	71	61
60	120	69	65	76	61	62	69
70	15	57	61	59	60	68	62
70	30	60	46	64	<b>69</b>	69	58
70	60	61	65	68	64	70	66
70	120	72	65	65	59	<b>72</b>	53
80	15	57	53	56	58	68	68
80	30	45	65	60	65	61	<b>72</b>
80	60	74	33	75	67	71	69
80	120	55	62	60	60	61	67
90	15	50	51	67	60	68	71
90	30	52	65	50	62	60	62
90	60	72	62	70	64	70	56
90	120	71	65	51	49	69	66

using Keithley 2400 in dark with thermally evaporated gold contacts on both surfaces of pellets in high vacuum  $10^{-6}$  Torr. The optical absorption spectra of the borate powders were taken by PerkinElmer UV–Vis spectrophotometer (PerkinElmer, MA, USA) at room temperature which dispersed in HCl solution in quartz tube. In order to determine the dielectric properties of the materials, pellets are gold coated on both surfaces using thermal evaporation technique under high vacuum to create a parallel plate capacitor structure. Dielectric measurements were taken using HP 4192A impedance analyser in the frequency range from 5 to  $1.3 \times 10^7$  Hz at room temperature.

## Results and discussion

### XRD results

From the XRD analysis, the results of raw materials and synthesized potassium borate are given in Table 2. According to Table 2, potassium source of KN is found as “nitre” with powder diffraction file (pdf) no. of “00-005-0377” and boron sources of H and B are found as “sassolite” and “boron oxide” with pdf no of “01-073-2158” and “00-006-0297”, respectively. Sodium and boron sources of T and Bx are found as “tinalconite” and “borax” with pdf nos of “00-007-0277” and “01-075-1078”, respectively. The synthesized potassium borate compound is found as “sassolite”

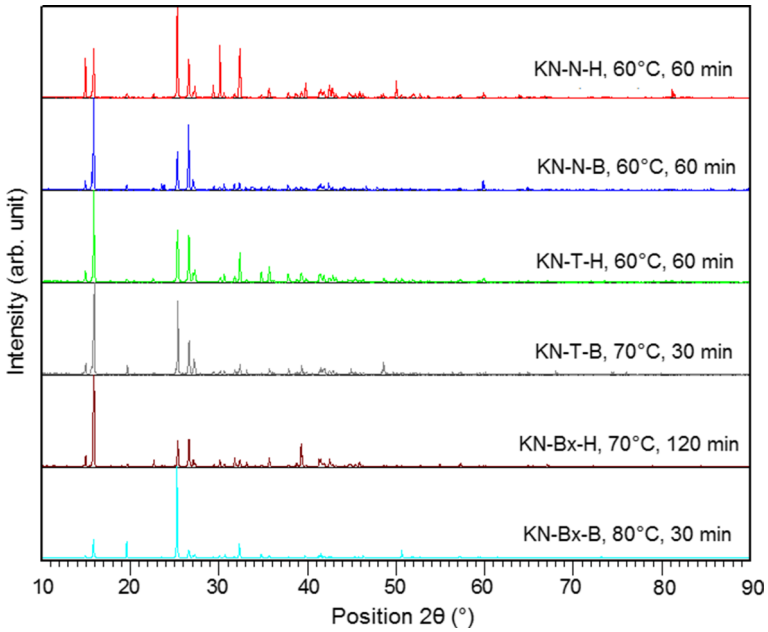


Fig. 1 XRD patterns of the optimum potassium borate phases

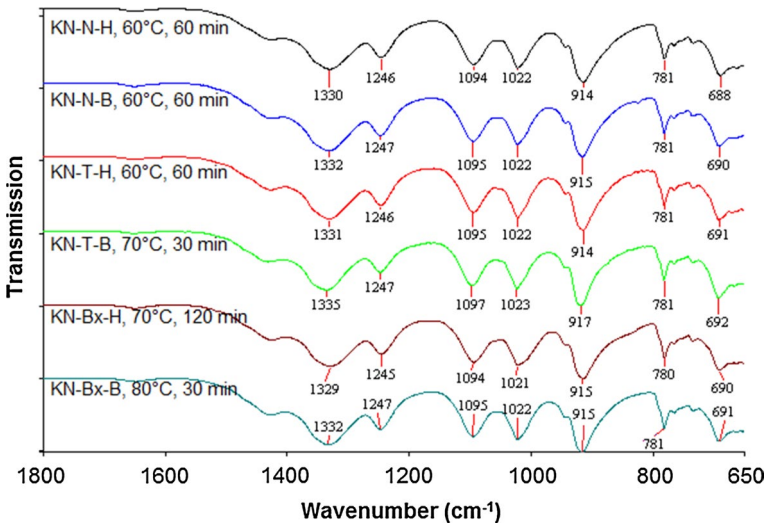


Fig. 2 FT-IR spectra of selected potassium borates

with pdf no. of “01-072-1688”. Synthesized type of a mineral is the same as in the study of Asensio et al. (2016) [6].

The XRD scores of the synthesized compounds are given in Table 3. The XRD score is the measure of the similarity of the theoretical compound meaning that when all the peak intensities (%) and peak locations are matched perfectly with the reference card, the XRD score of the analysed mineral is equal to 100 [6, 20].

The results of XRD analyses indicate the suitability of the hydrothermal conditions for the potassium borate synthesis. It is seen that the potassium borates are formed at different scores, in all the reaction parameters. The highest XRD scores are obtained at low reaction temperature and low reaction times. On the other hand, the changes in the reaction parameters are not affecting the crystal phase formation slightly. The highest XRD score is found as “77” at Set 3 with the reaction conditions of 60 °C and 60 min. On the other hand, in the study of Asensio et al. (2016), the highest XRD score was obtained at the reaction parameters of 60 °C and 15 min with the value of “74” from the raw materials of  $K_2CO_3$  and  $H_3BO_3$  [6].

In the first three sets, the highest XRD scores are obtained at the reaction parameters of 60 °C reaction temperature and 60 min of reaction time with the values of 75, 72 and 77. At the last three sets, the highest XRD scores are obtained at the reaction parameters of 70 °C–30 min, 70 °C–120 min and 80 °C–30 min with the values of 69, 72 and 72. These six highest XRD scored potassium borate minerals were determined as the optimum formations. The optimum formations for XRD patterns are given in Fig. 1.

In Fig. 1, the characteristic peaks (h k l [ $d_{\text{spacing}}$ ]) of santite were observed at the  $2\theta$  of 14.92° (1 1 1 [5.93 Å]), 15.85° (0 2 0 [5.59 Å]), 25.32° (0 2 2 [3.51 Å]), 26.59° (1 2 2 [3.35 Å]), 32.35° (4 0 0 [2.77 Å]) and 41.52° (4 2 2

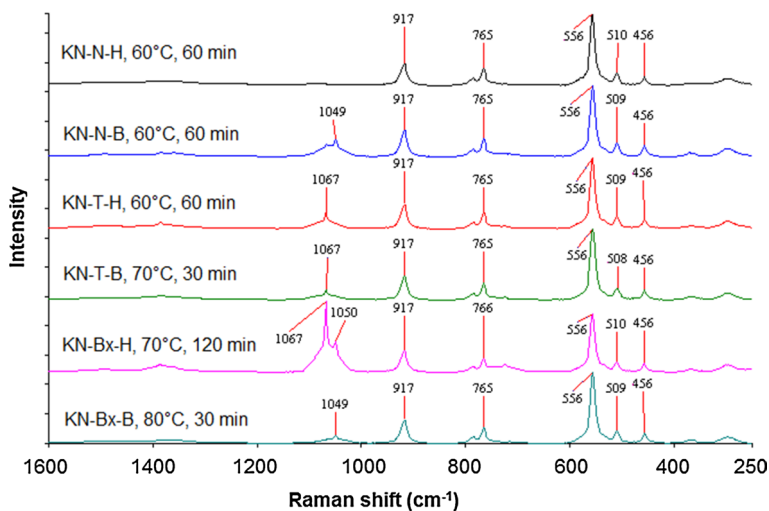
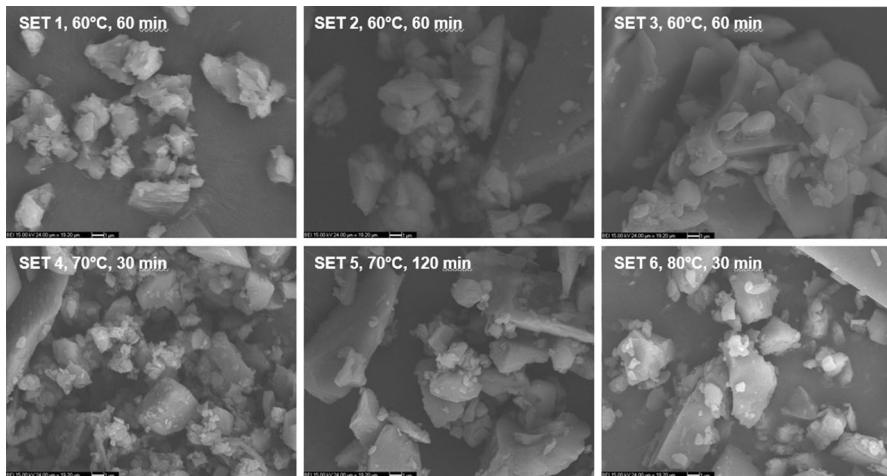


Fig. 3 Raman spectra of selected potassium borates





**Fig. 4** The surface morphologies of selected potassium borates

[2.17 Å]). These peak locations were in good agreement with the study of Asensio et al. (2016) [6].

### FT-IR and Raman spectroscopy results

FT-IR spectra of optimum potassium borate compounds are given in Fig. 2. For each reaction sets, the obtained FT-IR spectra of synthesized potassium borates showed similarity.

The peaks which are located between 1335 and 1329  $\text{cm}^{-1}$  are assigned to the asymmetric stretching of three coordinate boron to oxygen bands [ $\nu_{\text{as}}(\text{B}_{(3)}\text{-O})$ ]. The peaks in the range of 1247–1245  $\text{cm}^{-1}$  are attributed to the bending mode of boron-oxygen-hydrogen [ $\delta(\text{B-O-H})$ ]. The asymmetric stretching of four coordinate boron to oxygen bands [ $\nu_{\text{as}}(\text{B}_{(4)}\text{-O})$ ] is observed between 1097  $\text{cm}^{-1}$  and 1021  $\text{cm}^{-1}$ . The bands around 915  $\text{cm}^{-1}$  are related to the symmetric stretching of three coordinate boron to oxygen bands [ $\nu_{\text{s}}(\text{B}_{(3)}\text{-O})$ ]. The absorption peaks around 781  $\text{cm}^{-1}$  are due to the symmetric stretching of four coordinate boron to oxygen bands [ $\nu_{\text{s}}(\text{B}_{(4)}\text{-O})$ ]. The presence of IR peaks between 692  $\text{cm}^{-1}$  and 688  $\text{cm}^{-1}$  reveals the bending of three coordinate boron [ $\delta(\text{B-O-H})$ ].

In Fig. 3, Raman spectra of selected potassium borates are shown. According to Raman spectra, the bending of  $\nu_{\text{as}}(\text{B}_{(4)}\text{-O})$  is observed in the range of 1067–1049  $\text{cm}^{-1}$ , whereas the peaks at 917  $\text{cm}^{-1}$  are assigned to the symmetric stretching of  $\nu_{\text{s}}(\text{B}_{(3)}\text{-O})$ . The Raman frequencies around 765  $\text{cm}^{-1}$  belong to the symmetric stretching of  $\nu_{\text{s}}(\text{B}_{(4)}\text{-O})$ . The peaks at 556  $\text{cm}^{-1}$  attributed to the symmetric pulse vibration frequency of the pentaborate anion [ $(\text{B}_5\text{O}_6(\text{OH})_4)^-$ ]. The peaks which are shown as the bending of four coordinate boron  $\delta(\text{B}_{(4)}\text{-O})$  are seen between 510  $\text{cm}^{-1}$  and 456  $\text{cm}^{-1}$  [6, 21, 22]. These findings are in

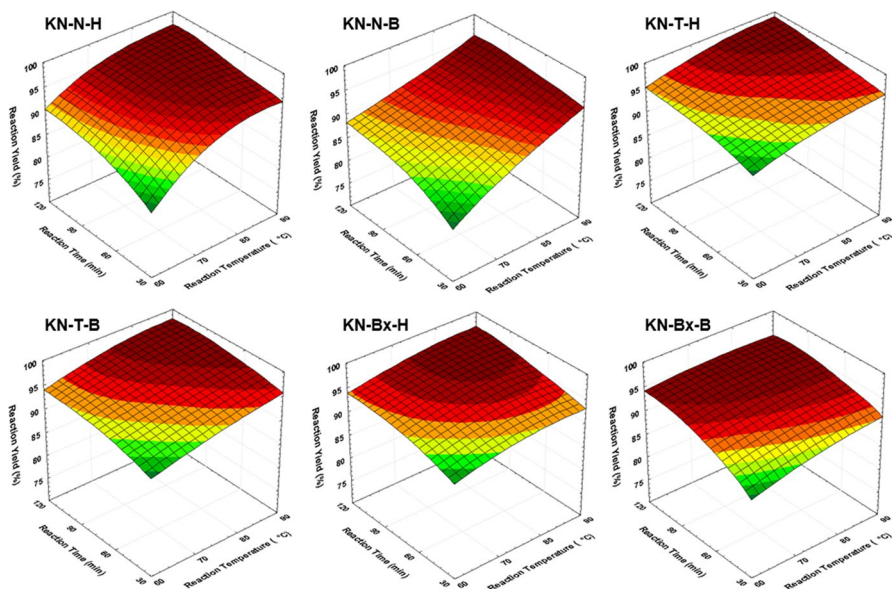


Fig. 5 Reaction yields of samples

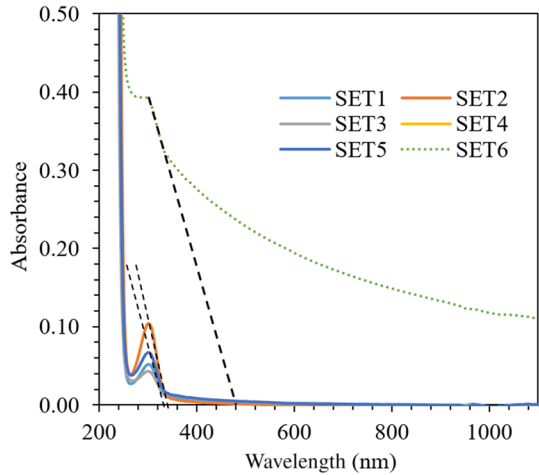
accordance with spectral characteristics of potassium borates which are obtained in the studies [6].

### SEM results

The surface morphologies of selected potassium borate samples are given in Fig. 4. According to SEM images of produced potassium borates, it is allowable that the morphology of products did not show a significant change based on precursor materials, reaction temperatures and reaction times. According to SEM images, the particle sizes of synthesized potassium borates were changed between 234.94 nm and 3.41  $\mu\text{m}$ . When uniform particle size distribution was observed for lower reaction temperatures and times, especially for Set 1, increasing reaction times and temperatures led to irregular particle morphologies.

The produced particles had the appearances of overlapped shapes in Set 2, whereas multiangular particles in Set 3. In Set 4, the particle size reduced to sub-micron scales but showed tendency to agglomeration. Irregular particle size distribution and morphology existed for Set 5 and Set 6, in which overlapped layers of potassium borate were observed.

**Fig. 6** The optical absorbance spectrum of potassium borates powders



**Reaction yields**

Reaction yields based on the santite formation are given in Fig. 5. All formations standard deviation is less than 5%. Considering all of these sets, the minimum santite yield was calculated as 76% in Set 2 at 60 °C and 15 min reaction time. As a comparison between the reactants of H<sub>3</sub>BO<sub>3</sub> and B<sub>2</sub>O<sub>3</sub>, highest santite yields were seen on H<sub>3</sub>BO<sub>3</sub>. This can be explained with the high incline to react of H<sub>3</sub>BO<sub>3</sub> than B<sub>2</sub>O<sub>3</sub>. Because B<sub>2</sub>O<sub>3</sub> was the anhydrous form of H<sub>3</sub>BO<sub>3</sub> and can be produced from H<sub>3</sub>BO<sub>3</sub>, where the reaction was given below:

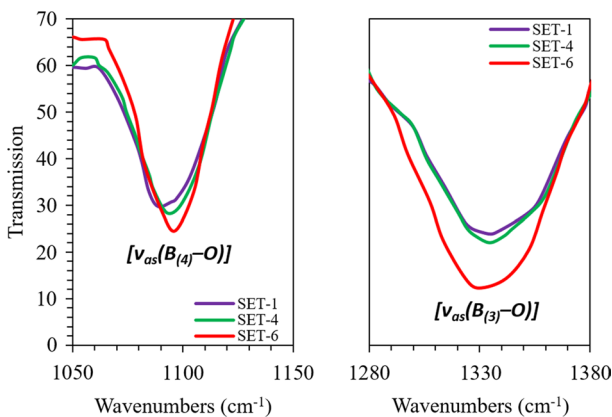
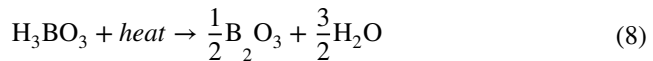


**Fig. 7** FT-IR spectra of selected potassium borates at about 1097 cm<sup>-1</sup> and 1332 cm<sup>-1</sup>

More likely for the comparison of  $\text{Na}_2\text{B}_4\text{O}_7 \cdot 5\text{H}_2\text{O}$  and  $\text{Na}_2\text{B}_4\text{O}_7 \cdot 10\text{H}_2\text{O}$ ,  $\text{Na}_2\text{B}_4\text{O}_7 \cdot 5\text{H}_2\text{O}$  as a reactant is more active than the  $\text{Na}_2\text{B}_4\text{O}_7 \cdot 10\text{H}_2\text{O}$ . This may be due to the boron percentages of the compounds since  $\text{Na}_2\text{B}_4\text{O}_7 \cdot 5\text{H}_2\text{O}$  has more boron percentage than the  $\text{Na}_2\text{B}_4\text{O}_7 \cdot 10\text{H}_2\text{O}$ . From the combination of both  $\text{Na}_2\text{B}_4\text{O}_7 \cdot 5\text{H}_2\text{O}$  and  $\text{H}_3\text{BO}_3$ , the highest santite yield was seen on the Set 3. Also the reactant of  $\text{NaOH}$  yields santite formation between  $\text{Na}_2\text{B}_4\text{O}_7 \cdot 5\text{H}_2\text{O}$  and  $\text{Na}_2\text{B}_4\text{O}_7 \cdot 10\text{H}_2\text{O}$ .

For the reaction temperatures and times, as it is seen from Fig. 5, santite yields were increased by the increase in both reaction temperature and time. The highest santite yield was obtained as 99% at Set 3 at 90 °C reaction time and 120 min reaction time. Higher santite formations were obtained than Asensio et al., 2016, which were between 84 and 95% [6].

### Optical and Electrical measurement results

The optical absorption spectra of the potassium borate powders synthesized using various boron minerals are shown in Fig. 6. The optical absorption edge was determined from extrapolation of the high-energy part of the absorption spectra and is shown in Fig. 6. The optical absorption edge of the potassium borate powders is observed at about 340 nm for Sets 1 to 5 and about 480 nm for Set 6.

In the structures of borate minerals and compounds, the differences in the  $\text{BO}_2$ ,  $\text{BO}_3$  and  $\text{BO}_4$  units are responsible for the different band gaps and other optical properties, which these units polymerize into superstructural motifs. The HOMO–LUMO band gap of  $\text{BO}_2$  is larger than that of  $\text{BO}_3$ , but smaller than that of  $\text{BO}_4$ .

The FT-IR spectra of the potassium borate Set 1, Set 4 and Set 6 at the peaks which are located between  $1335\text{--}1329\text{ cm}^{-1}$  and  $1097\text{ cm}^{-1}$ , the asymmetric

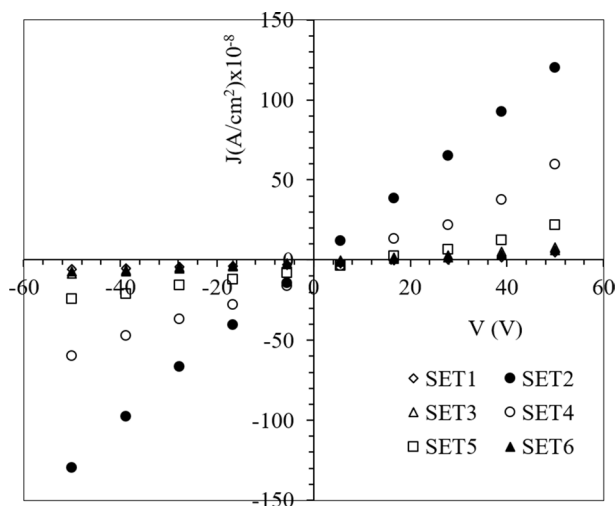


**Fig. 8** The DC current density–voltage characteristics of potassium borate materials synthesized using various boron minerals

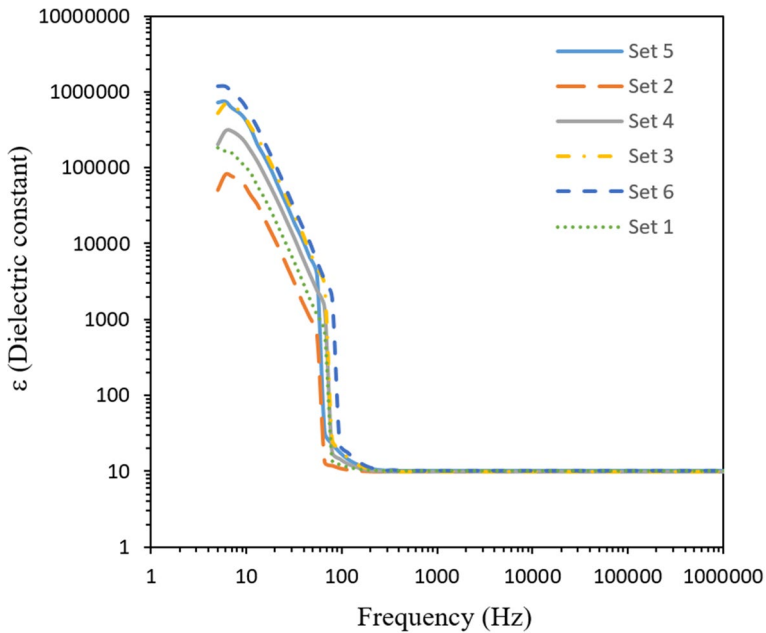
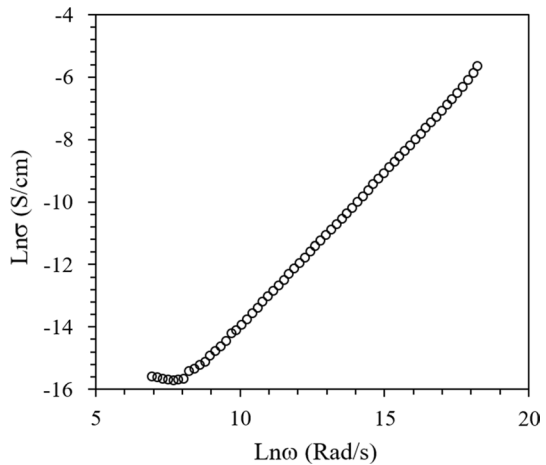


**Fig. 9** Frequency dependence of real part dielectric constant for potassium borates samples

**Fig. 10** Frequency dependence of AC conductivity for all about potassium borates samples



stretching of three coordinate boron to oxygen bands [ $\nu_{as}(B_{(3)}-O)$ ] and the asymmetric stretching of four coordinate boron to oxygen bands [ $\nu_{as}(B_{(4)}-O)$ ] are shown in Fig. 7, respectively. On the potassium borate samples, it was determined at about  $1332\text{ cm}^{-1}$  that the three coordinate boron asymmetric stretching to the oxygen bands for Sets 1–4 and 6 occurred.

While the amount of  $BO_4$  units in the spectra for Set 6 [7] did not change much, it was determined that  $BO_3$  units increased compared to other sets. This result causes

the absorption edges of the materials to shift to the near UV region, and the excess of  $\text{BO}_3$  units in Set 6 increases this shift.

However, properties such as crystal structure and crystalline size have a significant effect on the band gap. The amount of metal cations in the borate structure causes UV shift of the absorption edge, and the amount of O atoms in the B-O unit is also known to improve the use of the material for UV region applications [23].

The samples of the highest XRD scores are synthesized from various types of boron minerals, and the DC current density–voltage characteristics of these samples were determined using a standard technique. Figure 8 shows that the all potassium borate materials have high DC electrical resistance; these properties are valuable in terms of their ability to use materials as shielding. The bulk dc electrical resistivity of samples was determined in the range of  $4.17 \times 10^8$ – $4.07 \times 10^{10}$   $\Omega \cdot \text{cm}$  using the following equation:

$$R = \rho \frac{l}{A} \quad (9)$$

where R is the electrical resistance,  $\rho$  is the self-resistivity, A is the area of the sample surface, and l is the length.

Impedance spectroscopy is a widely used analysis method that provides information about the dielectric properties of materials. The dielectric properties of the materials were examined at different frequencies and at room temperature. The complex permittivity ( $\epsilon^*$ ) is given by the following equation:

$$\epsilon^* = \epsilon' - i\epsilon'' \quad (10)$$

where  $\epsilon'$  is the relative permittivity or dielectric constant and  $\epsilon''$  is the dielectric loss.

The dielectric constant and loss are calculated by Eq. (11):

$$\epsilon' = \frac{C_p d}{A \epsilon_0} \quad (11)$$

where d is the sample thickness, A is the surface area of the electrodes,  $\epsilon_0$  is the electrical permittivity of vacuum, and  $C_p$  is the capacitance of the sample.

Figure 9 shows the variation of the actual part of the dielectric constant depending on the frequency at room temperature. All materials showed very close dielectric constant and AC conductivity value and characteristic results. At low frequencies ( $5$ – $10^2$  Hz), the dielectric constant is high about  $2 \times 10^5$  to  $2 \times 10^6$  and decreases to about 10 with increasing frequency for all samples.

Figure 10 shows the similarly defined AC conductivity as approximate value and change in all type potassium borate materials as a function of frequency at room temperature. As shown in Fig. 9, a constant region indicating DC-like conductivity in the low-frequency region was observed and it was found that the conductivity increases with frequency starting from a limit frequency. The AC conductivity value in the DC-like region for materials is about  $1.7 \times 10^{-7}$  S/cm, and again from about 1 kHz, the exponential increasing ac conductivity region begins.

## Conclusion

In the present study, effects of using various raw materials, reaction temperatures and reaction times on the liquid state synthesis of potassium borates were examined. Also, electrical and optical properties of synthesized potassium borates were investigated. XRD results showed that santite ( $\text{KB}_5\text{O}_8 \cdot 4\text{H}_2\text{O}$ ) was synthesized at all the experimental sets. FT-IR and Raman spectra of products had characteristic potassium borate peaks in both IR and visible regions. The DC electrical resistivities of synthesized potassium borate materials are in the range of  $4.17 \times 10^8$ – $4.07 \times 10^{10}$   $\Omega \cdot \text{cm}$ . The dielectric constants were frequency dependent and varied between  $2 \times 10^5$  and  $2 \times 10^6$  at low frequencies ( $5$ – $10^2$  Hz), and about 10 at high frequencies. It was determined that the AC conductivity of the material depends on the frequency of  $10^3$  Hz sub-frequencies, in addition to the optical absorption edge of the potassium borate powders observed about 340 nm for Sets 1 to 5 and about 480 nm for Set 6.

**Authors contributions** MOA, FTSD and MYO carried out the experiments and wrote the MS, ASK and SAY conceived, carried out the experiments and wrote the MS, and EMD supervised the work and edited the manuscript.

**Funding** This work was not supported.

**Availability of data and material** made substantial contributions to the conception or design of the work; or the acquisition, analysis, or interpretation of data.

**Code availability** Not applicable.

**Declarations**

**Conflict of interest** Not applicable.

**Ethical approval** Not applicable.

**Consent to participate** Not applicable.

**Consent for publication** Not applicable.

## References

1. T.R. Prime Ministry SPO, Chemical Industry Private Expertise Commission, Boron Operations Group Report: Ninth Development Plan (2007–2013), Turkey (2006).
2. R. Beatty, *The Elements: Boron* (Marshall Cavendish, New York, 2005)
3. G. Yang, Z. Li, Y. Zhang, *Chem. Eng. Process.* **44**, 1216 (2005)
4. K. Thamizharasan, S.X. Jesu Raja, F.P. Xavier, P. Sagayaraj, *J. Cryst. Growth* **218**, 323 (2000).
5. S. Merlino, F. Sartori, *Contr. Mineral. Petrol.* **27**, 159 (1970)
6. M.O. Asensio, M. Yildirim, F. T. Senberber, A. S. Kipcak, E. Moroydor Derun, *Res. Chem. Intermed.*, **42**, 4859 (2016).
7. M. Mutailipu, K.R. Poepelmeier, S. Pan, *Chem. Rev.* **121**, 1130 (2021)

8. H.X. Zhang, J. Zhang, S.T. Zheng, G.Y. Yang, *Cryst. Growth Des.* **5**, 157 (2005)
9. C.G. Salentine, *Inorg. Chem.* **26**, 128 (1987)
10. Q. Wu, *Acta Cryst.* **E67**, i67 (2011)
11. G.M. Wang, Y.Q. Sun, S.T. Zheng, G.Y. Yang, Z. Anorg. Allg. Chem. **632**, 1586 (2006)
12. Z.H. Liu, P. Li, L.Q. Li, Q.X. Jia, *Thermochim. Acta* **454**, 23 (2007)
13. A. Alicilar, F. Ökenek, B. Kayran, M. Tutak, *J. Faculty Eng. Arch. Gazi Univ.* **30**, 701 (2015)
14. A.M. Abdel-Ghany, Ahmad S. Abu-Khadra, M.S. Sadeq, *J. Non Cryst. Solids.*, **548**, 120320 (2020).
15. B. Lyu, H. Li, L. Jiang, W. Shan, C. Hu, A. Deng, Z. Ying, L. Wang, Y. Zhang, H.B. Bechtel, M.C. Martin, T. Taniguchi, K. Watanabe, W. Luo, F. Wang, Z. Shi, *Nano Lett.* **19**, 1982 (2019)
16. M.I. Sayyed, Y.S. Rammah, F. Laariedh, A.S. Abouhaswa, T.B. Badeche, *J. Non Cryst. Solids.*, **527**, 119731 (2020).
17. S.N. Mohammad, Electrical characteristics of thin film cubic boron nitride. *Solid State Electron.* **46**, 203 (2002)
18. P. O. Ike, D. E. Folley, K. K. Agwu, M. L. Chithambo, S. Chikwembani, F. I. Ezema, *J. Lumin.*, **233**, 117932 (2021).
19. P. O. Ike, D. E. Folley, C. D. Umeh, K. K. Agwu, M. L. Chithambo, S. Chikwembani, F. I. Ezema, *J. Lumin.*, **226**, 117540 (2020).
20. T. Ibroska, A.S. Kipcak, S. Aydin Yuksel, E. M. Derun, S. Piskin, *Turk. J. Chem.*, 39, 1025 (2015).
21. J. Yongzhong, G. Shiyang, X. Shuping, L. Jun, *Spectrochim. Acta A* **56**, 1291 (2000)
22. L. Jun, X. Shuping, G. Shiyang, *Spectrochim. Acta A* **51**, 519 (1995)
23. S. Huang, C. Zhou, S. Cheng, F. Yu, *Chem Select* **4**, 10436 (2019)

**Publisher's Note** Springer Nature remains neutral with regard to jurisdictional claims in published maps and institutional affiliations.